Inorganic Chemistry

ARTICLE

pubs.acs.org/IC

Freezing in Resonance Structures for Better Packing: XeF_2 Becomes $(XeF^+)(F^-)$ at Large Compression

Dominik Kurzydłowski,*[,†] Patryk Zaleski-Ejgierd,[‡] Wojciech Grochala,[†,§] and Roald Hoffmann[⊥]

[†]Faculty of Chemistry, University of Warsaw, Pasteura 1, 02-093 Warsaw, Poland

[‡]Laboratory of Atomic and Solid State Physics and Cornell Center for Materials Research, Clark Hall, Cornell University, Ithaca, New York 14853-2501, United States

[§]Interdisciplinary Centre for Mathematical and Computational Modelling, University of Warsaw, Pawińskiego 5A, 02-106 Warsaw, Poland

[⊥]Baker Laboratory, Department of Chemistry and Chemical Biology, Cornell University, Ithaca, New York 14853-1301, United States

Supporting Information

ABSTRACT: Recent high-pressure experiments conducted on xenon difluoride (XeF_2) suggested that this compound undergoes several phase transitions up to 100 GPa, becoming metallic above 70 GPa. In this theoretical study, in contrast to experiment, we find that the ambient pressure molecular structure of xenon difluoride, of *I*4/*mmm* symmetry, remains the most stable one up to 105 GPa. In our computations, the structures suggested from experiment have either much higher enthalpies than the *I*4/*mmm* structure or converge to that structure upon geometry optimization. We discuss these discrepancies between experiment and calculation and point to an alternative interpretation of the measured cell vectors of XeF_2 at high pressure. At pressures exceeding those studied experimentally, above 105 GPa, the *I*4/*mmm* structure transforms to one of *Pnma* symmetry. The *Pnma* phase contains bent FXeF molecules, with unequal Xe−F distances, and begins to bring other fluorines into the coordination sphere of the Xe. Further compression of this structure up to 200 GPa essentially results in self-dissociation of XeF_2 into an ionic solid (i.e., $[XeF]^+F^-$), similar to what is observed for nitrous oxide (N_2O) at high pressure.

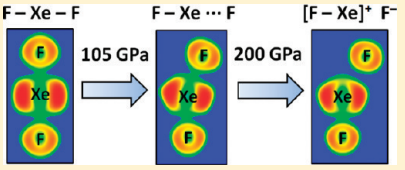

INTRODUCTION

Elements of group 18 (He, Ne, Ar, Kr, Xe, and Rn) were long considered as unable to form chemical bonds in neutral molecules, a prejudice refuted by the synthesis of the first noble gas compound by Bartlett in 1962.[1] After nearly half a century of superb (and difficult) experimental work, the chemistry of the heavier "noble gases" (Ar−Rn) is well developed.[2,3]

Xenon difluoride (XeF_2), among the simplest and most stable noble gas compounds, exhibits a rich chemistry, acting even as a ligand to metal centers.[3] This compound forms at room temperature an easily subliming, molecular solid consisting of linear XeF_2 units with two equal Xe−F bond lengths.[3,4] The *I*4/*mmm* crystal structure, central to our subsequent discussion, is shown in Figure 1. The linear molecular geometry is consistent with the VSEPR theory;[5] from the molecular orbital perspective, XeF_2 is a classical example of an electron-rich three-center system,[6] albeit one with a large share of ionicity.[7] The latter feature is due to significantly contributing ionic resonance structures, $[FXe]^+F^- \leftrightarrow F^-[XeF]^+$, proposed by Coulson.[8] These resonance forms also account for the fluoride donor properties of XeF_2, which is known to form XeF^+ salts.[9]

A recent high-pressure experiment conducted on solid XeF_2 indicated that this compound undergoes several phase transitions as the pressure is increased up to 100 GPa.[10] Starting from phase I (the ambient-pressure structure of *I*4/*mmm* symmetry; Figure 1) XeF_2 was found to transform to phase II (*Immm*) at 7 GPa and then to phase III (*Pnnm*-1[11]) at 13 GPa. The crystal structures of the two latter polymorphs can be derived from the *I*4/*mmm* structure by a slight modification of its cell vectors; both of them contain symmetric and linear XeF_2 molecules in the same arrangement as that in *I*4/*mmm*. Above 23 GPa, phase IV is observed, which is semiconducting, in contrast to the electrically

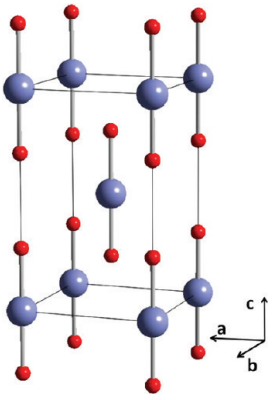

Figure 1. Ambient-pressure polymorph of XeF_2 of *I*4/*mmm* symmetry. Blue/red balls mark Xe/F atoms.

Received: February 22, 2011
Published: March 25, 2011

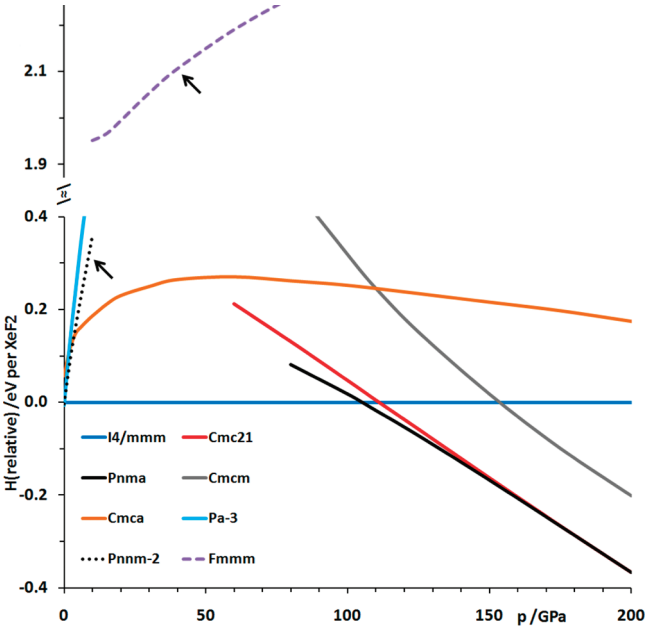

Figure 2. Relative enthalpy at 0 K per XeF_2 unit (referenced to that of *I4/mmm*) of selected high-pressure polymorphs of XeF_2 (for a plot depicting all polymorphs studied, see the SI). Arrows mark the enthalpy dependence of the structures proposed in the previous high-pressure experiment.[10] Note the *I4/mmm* to *Pnma* transition at 105 GPa.

insulating phases I–III. This polymorph (*Pnnm*-2, isomorphic to β-KrF_2[12]) also contains linear XeF_2 units, but these are arranged in graphite-like layers.[10] It is supposed that phase IV transforms at ~70 GPa to a metallic phase V, a fluorite-like (ionic) structure of *Fmmm* symmetry.

In this work, we present a theoretical investigation into the stability of various polymorphs of XeF_2 at high pressure. In contrast to the experimental results, our density functional theory (DFT) calculation indicates that the ambient-pressure *I4/mmm* structure persists as the thermodynamically most stable phase of xenon difluoride up to 105 GPa. Our computations indicate that above this pressure bending and bond-length differentiation within the XeF_2 units should lead to the emergence of a new phase of *Pnma* symmetry (evolving to *Cmcm*), which is metallic and stable up to at least 200 GPa. At pressures exceeding 200 GPa, the *Pnma* structure, while metallic, contains isolated $[XeF]^+$ units separated by F^- anions. The picture that emerges suggests self-dissociation of XeF_2 promoted by high pressure.

RESULTS AND DISCUSSION

Computed Polymorphs of XeF_2. In the present study, a vast range of structures, which can be divided into three categories, has been screened in the pressure range from 0 to 200 GPa.[13] The first group contains xenon difluoride polymorphs derived from the already known structures of ABB′ compounds: (i) ternary compounds containing a divalent metal and two halogens (e.g., HgClBr) or ones containing a trivalent metal, oxygen, and a halogen (e.g., FeOCl); (ii) ambient- and high-pressure molecular phases of CO_2[14] and high-pressure phases of N_2O.[15] The second group consisted of the high-pressure phases I–V of XeF_2 suggested by Kim et al.[10] Finally, the third category encompasses structures obtained from the application

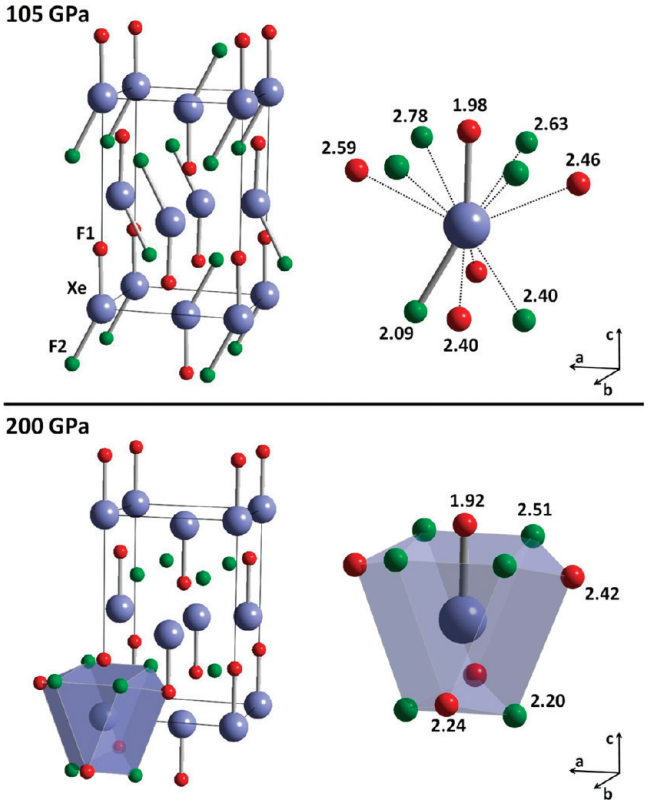

Figure 3. Crystal structure and coordination of Xe in *Pnma* at 105 GPa (top) and 200 GPa (bottom). Blue balls mark Xe atoms, and red/green balls mark F1 and F2 atoms, respectively. Gray lines mark contacts in the first coordination sphere of Xe, while dashed lines/blue polyhedra mark contacts in the second coordination sphere at 105 and 200 GPa, respectively. Distances between Xe and F atoms are given in angstroms. The structures are shown with the cell origin shifted by (0.261·**a**, 0.25·**b**, 0.030·**c**) at 105 GPa and by (0.25·**a**, 0.25·**b**, 0.034·**c**) at 200 GPa. At 200 GPa, the actual space group symmetry is higher, *Cmcm*.

of a genetic algorithm for structure searching, implemented in the *USPEX* program.[16]

We choose to reference the enthalpies of various structures at each pressure point to that of the ambient-pressure polymorph of XeF_2 (phase I, *I4/mmm*). Surprisingly (given the experimental findings cited), in our calculations this structure turned out to be the most stable one up to a pressure as high as 105 GPa (Figure 2). Moreover, it does not exhibit imaginary phonon modes in the whole pressure range studied (i.e., up to 200 GPa). At 105 GPa, the *I4/mmm* phase can still be described as a molecular crystal with two short Xe–F bonds at 1.99 Å and eight secondary contacts at 2.52 Å (details will be shown below). In maintaining its molecular structure upon compression, XeF_2 resembles nitrous oxide (N_2O), which at ambient temperature and high pressure remains molecular up to 135 GPa.[15d] As we will see, there is another similarity in the high-pressure behavior of XeF_2 and N_2O.

The previously reported nonmolecular high-pressure phases of XeF_2, phases IV and V,[10] have much higher enthalpy than *I4/mmm* (*Pnnm*-2 and *Fmmm*, respectively, shown in Figure 2). They also exhibit substantial phonon instabilities, i.e., imaginary phonon frequencies. Suggested phases II (*Immm*) and III (*Pnnm*-1) converged to the *I4/mmm* structure after geometry optimization at ambient and high pressure. Not surprisingly, molecular polymorphs of XeF_2 isostructural with high-pressure phases of CO_2

dx.doi.org/10.1021/ic200371a |*Inorg. Chem.* 2011, 50, 3832–3840

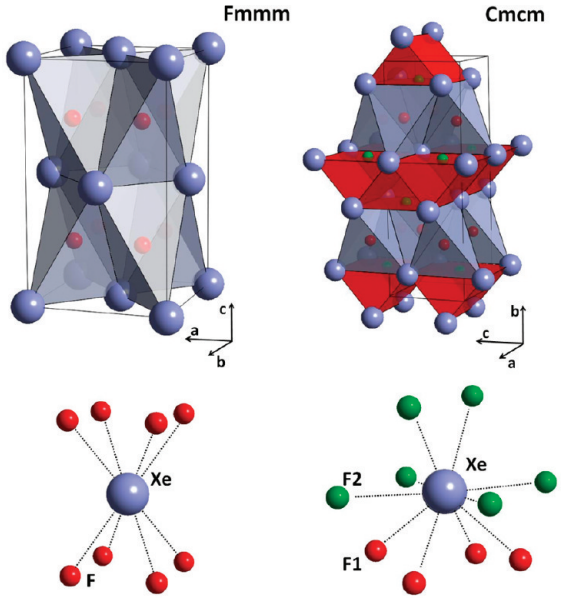

Figure 4. Crystal structure and coordination of Xe at 105 GPa for *Fmmm* (left) and *Cmcm* (right). Blue balls mark Xe atoms, and red and green balls mark F atoms (in *Cmcm*, red and green balls mark F1 and F2 atoms, respectively). Blue/red polyhedra mark the coordination of fluorine in the CaF_2-type/CsCl-type layers.

(*Cmca* and $Pa\bar{3}$[14]) are of nearly the same enthalpy as *I*4/*mmm* at 0 GPa, but upon compression, they are destabilized with respect to *I*4/*mmm* due to the less efficient packing of XeF_2 units.[17]

Above 105 GPa, two new, closely related structures become more stable than the *I*4/*mmm* one. These are *Pnma* and $Cmc2_1$ found in our *USPEX* calculations. They merge into each other at higher pressures, and from now on, we will refer to the pair as *Pnma*. At 105 GPa, this structure can be described as approximately molecular, as shown in Figure 3. It contains bent F−Xe−F entities with two unequal Xe−F distances. The second coordination sphere of Xe is considerably altered compared to *I*4/*mmm*; as one can see in Figure 3, four F atoms comes closer than 2.50 Å to a Xe.

It should be said that the bonding in this *Pnma* polymorph evolves upon compression, as shown in the 200 GPa structure in Figure 3. First, its symmetry increases to *Cmcm*; Figure 3 (bottom) clearly shows the additional mirror planes in the structure. Second, in the *Pnma* structure at 200 GPa, one of the bonds of the F−Xe−F entity elongates (2.09−2.20 Å), while the other contracts (1.98−1.92 Å). After the 1.92 Å primary bond, there are now four secondary Xe−F contacts shorter than 2.25 Å. We will present below a detailed argument for considering this structure as an ionic crystal of $[XeF]^+F^-$ stoichiometry. Also, we will follow the transformation between *I*4/*mmm* and *Pnma* in more detail.

As was already mentioned, the previously postulated "fully" ionic $Xe^{2+}[F^-]_2$ *Fmmm* polymorph, a CaF_2-type structure,[10] has an enthalpy over 2.2 eV higher than that of *I*4/*mmm* at 80 GPa (Figure 2). The best "fully" ionic structure found in our study is the *Cmcm* polymorph derived from *USPEX* calculations (Figure 4), which becomes thermodynamically more stable than *I*4/*mmm* above 154 GPa (but still substantially less stable than *Pnma*; Figure 2).

Interestingly, this structure exhibits fluorite layers resembling those found in CaF_2 but separated by CsCl-type sheets. Such an arrangement of atoms leads to an increase of the coordination number of Xe from 8 in *Fmmm* to 10 in *Cmcm*: the latter polymorph

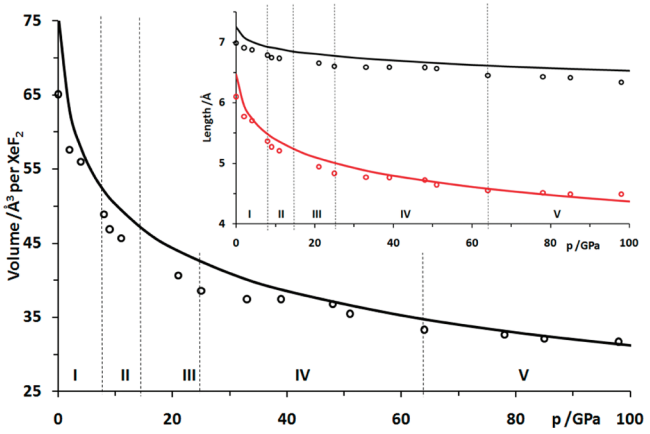

Figure 5. Calculated compressibility of *I*4/*mmm* (black line) compared with experimental points (black circles). Inset: pressure dependence of **a** and **c** cell vectors of the face centered cell of *I*4/*mmm* (red and black lines, respectively); red/black circles mark experimental **a** and **c** lattice parameters of phases I−V transformed to an analogous face centered cell (see the text). Vertical dashed lines indicate experimental stability regions of phases I−V.

is then much more compact and, therefore, more stable at high pressure. The relationship may be gleaned from a side-by-side comparison of the unstable *Fmmm* structure and our *Cmcm* one in Figure 4.

Probing the Disagreement of Experiment and Theory. Before we move on to a more detailed description of what happens with XeF_2 above 100 GPa, we suggest a potential reconciliation of the disagreement between theory and experiment that has emerged. As was already indicated in the preceding section, the experimental *Pnnm*-2 and *Fmmm* structures are not plausible candidates for high-pressure polymorphs of XeF_2 because of their high enthalpy and dynamic instability. We also find that the ambient-pressure structure of xenon difluoride persists as the most stable polymorph up to 100 GPa, whereas four phase transformations in this pressure range were reported by Kim et al., based on resistivity measurements, Raman spectroscopy, and powder X-ray diffraction (PXRD).[10]

Let us compare the structural data obtained from X-ray scattering with the calculated structural features of the *I*4/*mmm* polymorph of XeF_2 (denoted as phase I by Kim et al.[10]). First of all, we notice (Figure 5) that the calculated volume versus pressure dependence for *I*4/*mmm* is in good agreement with the experimental compressibility of all previously reported phases of XeF_2.

Surprisingly, the biggest differences are found for phases II and III, which are almost identical with phase I and which (in the calculations) converge to this high-symmetry *I*4/*mmm* polymorph upon geometry optimization. The compressibility of the nonmolecular phase V is in almost perfect agreement with that calculated for *I*4/*mmm*. Upon careful inspection of the experimental structures, we find one more striking similarity between *I*4/*mmm* and phases II−V of XeF_2. Namely, in all of those polymorphs, the Xe atoms form a fcc-type sublattice, clearly seen, for instance, in *Fmmm* in Figure 4. Therefore, one can transform the unit cells of phases I−V into a common face centered cell. This is done in Figure 6, enabling a direct comparison of the cell vectors of all phases, as is shown in the inset of Figure 5. From that comparison, one can see that the calculated pressure dependence of the **a** and **c** cell vectors of *I*4/*mmm* is in

dx.doi.org/10.1021/ic200371a |*Inorg. Chem.* 2011, 50, 3832–3840

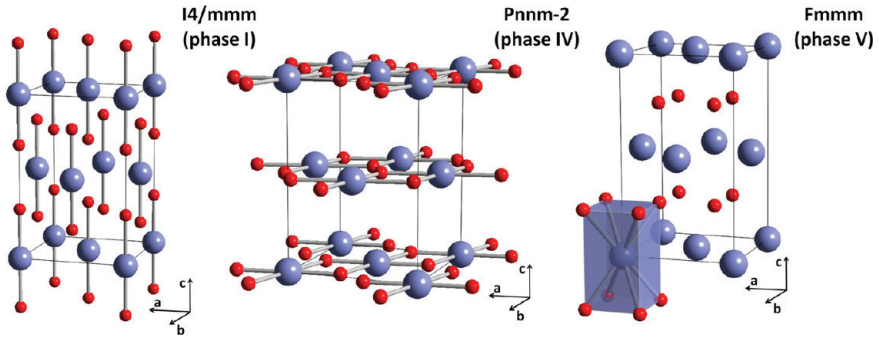

Figure 6. Experimental structures of XeF_2: *I4/mmm* (phase I), *Pnnm*-2 (phase IV), and *Fmmm* (phase V). Blue/red balls mark Xe/F atoms. *I4/mmm* and *Pnnm*-2 are shown in a nonstandard face centered cell.[18] Phases II (*Immm*) and III (*Pnnm*-1) are not shown because they differ from *I4/mmm* only by cell vector lengths.

good agreement with experiment not only in the stability region of phase I but up to 100 GPa.

These considerations lead us to the conclusion that the only difference among phases II−V and *I4/mmm* lies in the positioning of F atoms in the unit cell. In the experiment, the fractional coordinates of these atoms were obtained by Rietveld refinement of the PXRD pattern. The X-ray scattering power of a given atom is proportional to Z^2, where Z is the atomic number. Given the large differences in the atomic number between Xe ($Z = 54$) and F ($Z = 9$), the majority of the peak intensity originates from scattering of the heavier atom. Obtaining fluorine positions from X-ray measurements of XeF_2 is thus a nontrivial task. Moreover, powder samples squeezed between two diamonds can exhibit the preferred orientation of the crystallites, which, in turn, can perturb the intensity of the observed peaks.

Without making any judgment on the quality of the PXRD data presented in ref10, we conclude that the discrepancies between the computational evidence presented here and the experimental results call for a renewed effort in establishing the high-pressure structural behavior of XeF_2. Especially, extending the measured pressure range beyond 100 GPa seems to be vital in order to verify the possible existence of the *Pnma* structure.[19]

Distortions of XeF_2 at High Pressure. Now we move on to the transition between *I4/mmm* and *Pnma*, which takes place above 105 GPa.

Looking at the structures of these polymorphs, one, in fact, perceives several similarities. Thus, the *Pnma* phase can be derived from the *I4/mmm* structure (transformed to a face centered cell, as shown in Figure 7) by a concerted movement along the **a** vector of half of the F atoms [see the Supporting Information (SI) for animation], the ones that we mark F2 in *Pnma*. This results in the previously mentioned bond-length difference within the F−Xe−F unit (with the Xe−F2 bond being the longer one; see Figure 7) and bending of the F−Xe−F angle, to 153° at 105 GPa.[20] We note that the bending vibration and asymmetric stretch of the free XeF_2 molecule have relatively low frequencies of only 212 and 560 cm^{-1}, respectively.[21] This indicates that the high symmetry of the XeF_2 unit can be easily violated, as seen in the case of the *I4/mmm* to *Pnma* transition. Application of the above-mentioned distortions to *I4/mmm* at 105 GPa leads to a structure of *Pnma* symmetry, with the cell origin shifted from the standard setting by (0.261·**a**, 0.25·**b**, 0.030·**c**). The transition between the two polymorphs is associated with a volume collapse of 1.8% at 105 GPa, with the number of F atoms in the coordination sphere of Xe increasing from 10 in *I4/mmm* to 11 in *Pnma*.

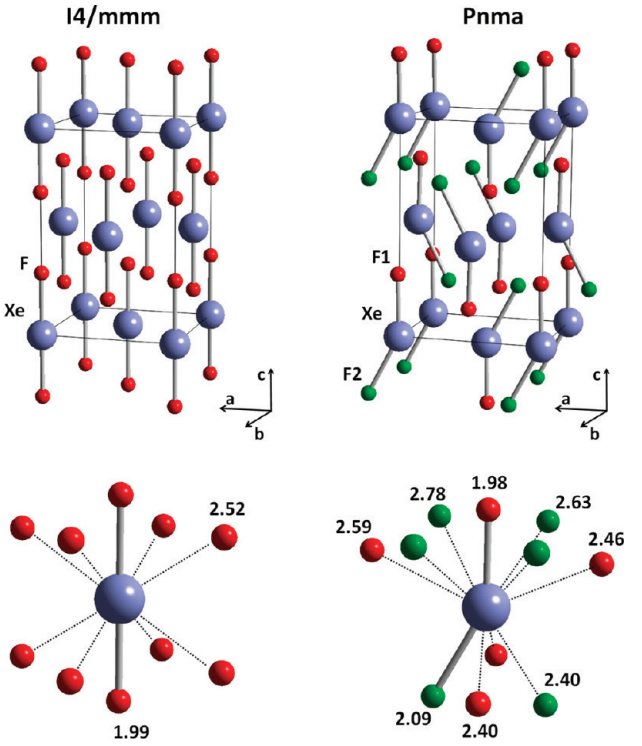

Figure 7. Crystal structure of XeF_2 and coordination of Xe in *I4/mmm* (left) and *Pnma* (right) at 105 GPa. Blue balls mark Xe atoms, and red and green balls mark F atoms (in *Pnma*, red/green balls mark F1/F2 atoms). Gray lines/dashed lines mark contacts in the first/second coordination sphere of Xe. Distances between Xe and F atoms are given in angstroms. The *I4/mmm* structure is shown in a nonstandard face centered cell,[18] while for *Pnma*, the cell origin is shifted by (0.261·**a**, 0.25·**b**, 0.030·**c**).

The *Pnma* structure at 105 GPa has two short Xe−F bonds (1.98 and 2.09 Å) that can be distinguished from nine secondary Xe···F contacts in the range 2.40−2.78 Å (Figure 3). This polymorph can then be seen as a distorted version of *I4/mmm*, with the distortion localized mainly within the XeF_2 unit, which is both bent and unsymmetrical. Upon compression, the two structures become more dissimilar. For *I4/mmm*, all nearest-neighbor and second-nearest-neighbor distances contract upon compression, in such a way that at 200 GPa this structure still looks like a molecular crystal, with two short Xe−F bonds at 1.952 Å and eight secondary contacts at 2.375 Å.[22]

dx.doi.org/10.1021/ic200371a |*Inorg. Chem.* 2011, 50, 3832–3840

Quite in contrast, compressing *Pnma* leads to an elongation of the Xe−F2 bond in the F1−Xe−F2 unit. It increases from 2.09 Å at 105 GPa to 2.20 Å at 200 GPa, at which point it becomes equal to the shortest Xe···F2 secondary contact (see the bottom of Figure 3). At the same time, the Xe−F1 bond contracts from 1.98 to 1.92 Å. As a consequence, at 200 GPa, the first coordination sphere of Xe in *Pnma* consists of only one short chemical bond (Xe−F1), with the remaining 10 contacts forming a complex undecahedron (Xe−F distances 2.20−2.51 Å) depicted at the bottom of Figure 3. Interestingly, the orientation of the undecahedron is such that there are no Xe···F contacts present in the plane perpendicular to the Xe−F1 bond. This would indicate that *Pnma*, like the ambient-pressure *I*4/*mmm* structure, minimizes the repulsive interaction between Xe lone-pair electrons (forming a torus around the Xe atom) and lone-pair electrons residing on neighboring F atoms. The fact that such interactions play a significant role even at high pressure has been nicely demonstrated in the case of stereochemically active electron pairs of Tl^+ and Pb^{2+}.[23]

High-Pressure Self-Dissociation. Dividing the coordination sphere of Xe in *Pnma* at 200 GPa (Figure 3) into the short Xe−F1 bond (1.92 Å) and the other Xe···F contacts (2.20−2.51 Å) may seem artificial but, as we argue, makes sense in several ways. First, we note that if the [XeF1] unit is replaced by a single atom located at the center of mass of this entity, the resulting arrangement of atoms can be described as a distorted anti-NiAs structure, with the remaining F2 atoms occupying the anion positions.[24] This suggests that *Pnma* at 200 GPa may be viewed as a structure built up from $[XeF]^+$ and F^- ions. This, in turn, could be rationalized in terms of the Coulson model,[8] as a shift of the balance of the $[FXe]^+F^- \leftrightarrow F^-[XeF]^+$ resonance toward one of the resonance structures, and would explain the shortening of the Xe−F1 bond in *Pnma* with respect to the Xe−F bond in *I*4/*mmm*. This would be the consequence of formation of the more strongly bound XeF^+, which has a full Xe−F bond, while Xe−F in XeF_2 has a weaker three-center bond. The Xe−F bond length in XeF^+ in $(XeF)(AsF_6)$ is 1.89 Å[4d] and that in $(XeF)(SO_3F)$ is 1.94 Å,[9b] while the Xe−F bond length in XeF_2 is 2.00 Å.[4d]

The above-mentioned observations lead us to describe the changes seen in *Pnma* at compression as a process of self-dissociation of XeF_2 (i.e., $XeF_2 \rightarrow XeF^+ + F^-$). We note that there exist a number of phase transformations from a molecular to ionic crystal upon compression. Partial ionization at high pressure has been claimed even for pure elements forming covalent networks, such as B.[25] In the case of molecular species, full ionization (involving a change in the formal oxidation state) has been previously reported for N_2O, which at high pressure and temperature liberates N_2 and forms nitrosonium nitrate ($NO^+NO_3^-$) with a structure closely resembling that of $CaCO_3$.[15a−c] The unusual result clearly requires much chemistry along the reaction path; the mechanism of this transformation is not yet known. Nitrous oxide is a linear molecule, in a way related to XeF_2 in that it is often described by two resonance structures: $N{\equiv}N^+O^- \leftrightarrow N^-{=}N^+{=}O$. We also note that ammonia has been predicted to disproportionate at high pressure into ammonium amide ($NH_4^+NH_2^-$).[26]

Another connection can be drawn between the *Pnma* polymorph and the ambient-pressure structures of compounds in which the XeF_2 molecule acts as a fluoride donor (Lewis base). In fact, compounds containing XeF^+ species can be obtained upon the reaction of XeF_2 with strong fluoride ion acceptors (e.g., AsF_5, SbF_5).[3] For instance, in the aforementioned XeF^+-$[AsF_6]^-$[25] Xe is coordinated by two F atoms at 1.87 and 2.21 Å. The longer distance is to a F best described as an integral part of an AsF_6^- anion. Actually, what we see here is a common feature of all hypervalent compounds.[27] This is illustrated by plotting the short and long bond lengths of the distorted XeF_2 entity on one graph, a classical Bürgi−Dunitz plot.[28] This has been done in Figure 8 for a handful of ambient-pressure XeF_2 compounds, along with the *Pnma* structure at high pressure. We notice that the pressure dependence of the Xe−F1 and Xe−F2 bond lengths of the F1−Xe−F2 entity in *Pnma* fits in very nicely with the variation noticed in the ambient-pressure structures.

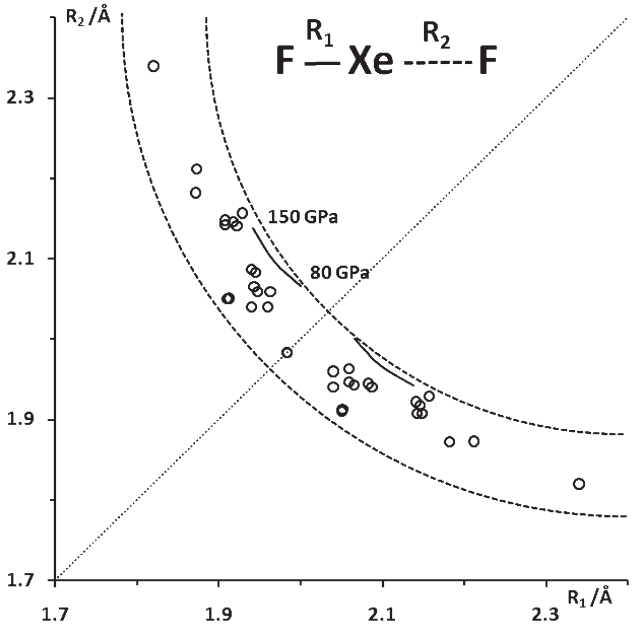

Figure 8. Bond alternation within the XeF_2 entity for ambient-pressure compounds (black circles) and *Pnma* at high pressure (black line). The (R_1, R_2) points are copied on the other side of the $R_1 = R_2$ dotted line. Dashed lines are guides for the eye.

From the above, it seems that for XeF_2 high pressure accomplishes the same job as strong Lewis acids do at ambient conditions: it freezes this molecule into one of its resonance structures. It is worth pointing out that in the gas phase this process is thermodynamically highly unfavorable: the enthalpy of the reaction $XeF_2(g) \rightarrow XeF^+(g) + F^-(g)$ is 9.72 eV,[4d] while the lattice energy of a hypothetical $[XeF^+]F^-$ salt is only 7.15 eV per formula unit (see the SI). Hence, at ambient conditions, one needs a strong fluoride ion acceptor to produce XeF^+, as exemplified by AsF_5 with its experimental F^- ion affinity of 4.36 (±0.23) eV from thermodynamic considerations[29] (4.59 eV from ab initio calculations[30]).

The perspective of self-dissociation of XeF_2 in *Pnma* finds confirmation in an analysis of the electron localization function (ELF)[31] calculated for both the *Pnma* and *I*4/*mmm* polymorphs at high pressure (Figure 9). High ELF values (close to 1, which is the upper limit of this function) indicate paired electrons (i.e., lone pairs, bonds, and core electrons), whereas values around 0.5 point to electrons that behave as in a uniform electron gas.[34] Not surprisingly, for XeF_2, the highest ELF values are found in the region of Xe and F lone pairs (core electrons are not seen in Figure 9 because they are omitted in pseudopotential calculations).

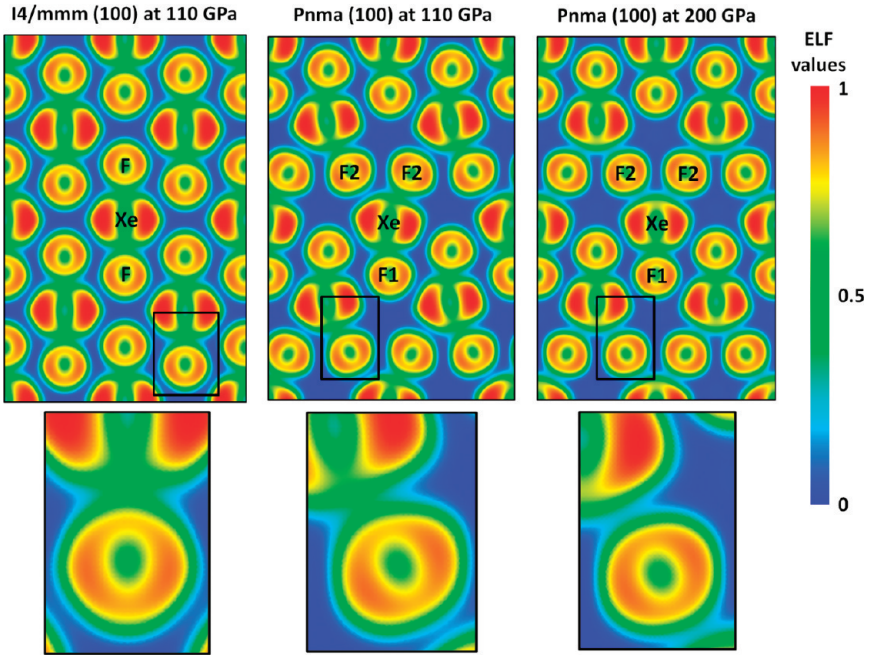

Figure 9. (100) cross section of ELF for *I*4/*mmm* at 110 GPa and *Pnma* at 110 and 200 GPa. The positions of Xe and F atoms are also shown for clarity.

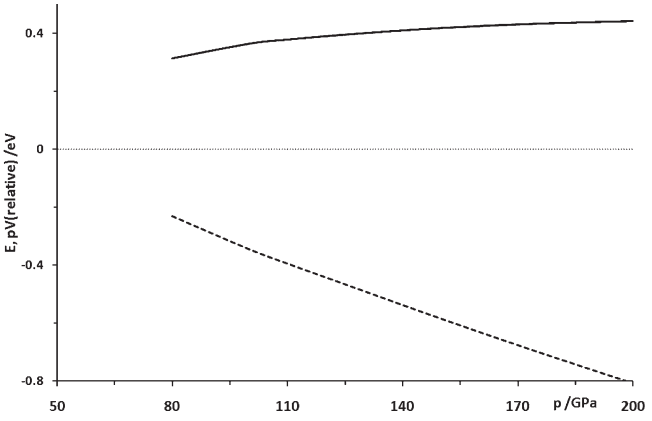

Figure 10. Relative energy (solid line) and the *pV* term (dashed line) per XeF_2 unit of the *Pnma* phase with respect to *I*4/*mmm*.

In the (100) section of *I*4/*mmm* at 110 GPa, one can see moderate ELF values in the region of the Xe−F bond. The distortion leading to *Pnma* results in a decrease of the ELF values along the Xe−F2 bond, as can be seen in the (100) section of *Pnma* at 110 GPa (Figure 9, middle). At 200 GPa, the Xe and F2 ELF basins become virtually disconnected (i.e., few paired electrons reside at the Xe···F2 contact). This corroborates the notion that the application of high pressure leads to an increase of the ionicity of one of the Xe−F bonds and subsequent effective self-dissociation into isolated $[XeF^+]$ cations and F^- anions at 200 GPa.

What is the driving force responsible for the transition to the self-dissociated structure of XeF_2 at high pressure? No doubt it is the volume collapse upon moving from a molecular to an ionic solid. Indeed, inspection of the internal energy and the *pV* term of *Pnma*, referenced to that of *I*4/*mmm* (Figure 10), clearly shows that it is the *pV* term that makes *Pnma* more stable than *I*4/*mmm* at high pressure. Better packing in the *Pnma* structure is reached by differentiation of the sizes of the F atoms: the anionic F2 is "larger" (coordinated by six Xe atoms at a mean distance of 2.41 Å at 200 GPa), while F1 is "smaller" (it has five contacts to Xe; mean distance 2.25 Å at the same pressure) compared to the F atoms in *I*4/*mmm* (five contacts; mean 2.29 Å).

Electronic Structure of XeF_2 under Pressure. The *I*4/*mmm* polymorph of XeF_2, at the origin of our story, is a colorless wide-band-gap insulator at ambient pressure. However, the electronic properties usually change a great deal when matter is subject to megabar pressures. We find that the band gap in *I*4/*mmm*, equal to 2.76 eV at 0 GPa, closes at 60 GPa. This calculated pressure of the metallization of XeF_2 is thus in fair agreement with the experimental value of 70 GPa.[10]

The electronic density of states (DOSs) calculated for the *I*4/*mmm* structure at 110 GPa, when it is metallic and just about to transform to *Pnma*, are shown in Figure 11. The lower bands are F 2s and Xe 5s in nature; near the Fermi level, the states are a mixture of F 2p and Xe 5p (see the SI). In fact, the band-gap closure in *I*4/*mmm* is due to the overlap of p-type bands originating from the occupied π^* and unoccupied σ^* orbitals of the XeF_2 molecule. In the *Pnma* structure, the F s band is now split into two groups, which can be attributed to the 2s states of F1 and F2. The bands originating from F2 s states are destabilized with respect to the F1 band; they also have a smaller dispersion, as can be seen in Figure 11. Those differences are consistent with the fact that the former atoms are, in fact, negatively charged F^- moieties, while the latter constitute a part of the XeF^+ cation. One might argue that metallization of the *I*4/*mmm* polymorph (connected with partial transfer of the electron density from weakly antibonding π^* to much more antibonding σ^*) has set the ground work for the *I*4/*mmm* → *Pnma* phase transition; as the occupation of σ^* states increases in the 70−110 GPa pressure range, the system has a choice of whether to continue filling the σ^* states (which inevitably leads to a weakening of both Xe−F bonds) or rather to sacrifice one of the bonds and strengthen the

dx.doi.org/10.1021/ic200371a |*Inorg. Chem.* 2011, 50, 3832–3840

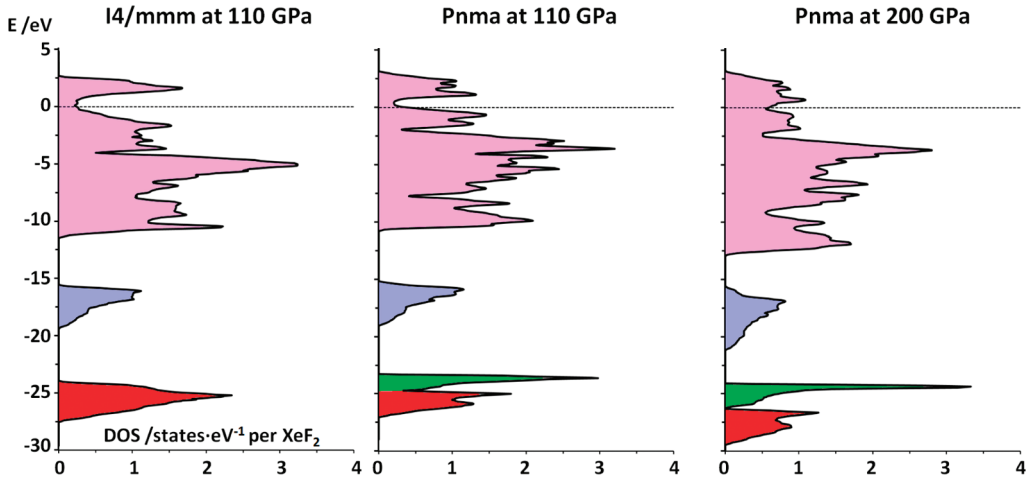

Figure 11. Total electronic DOSs of *I*4/*mmm* at 110 GPa (left) and *Pnma* at 110 GPa (center) and 200 GPa (right). The energy of the Fermi level has been set to zero. Colors *schematically* indicate the following bands: F 2s (red and green; for *Pnma*, red/green marks bands originating from F1/F2), Xe 5s (blue), and a mixture of F 2p and Xe 5p (pink). For partial DOS calculations, see the SI.

other. The outcome is that the phase transition takes place at $p >$ 110 GPa, with XeF_2 detaching one F to pack better.

Although *I*4/*mmm* is metallic at 110 GPa, it still exhibits a pseudogap, and consequently the DOS at the Fermi level is low. It increases upon transition to *Pnma* because in that structure the pseudogap is smaller (Figure 11). Upon compression of *Pnma*, it diminishes and eventually disappears at 200 GPa. This is associated with a 3-fold increase of the Fermi level DOS from 110 to 200 GPa. We note that the bands crossing the Fermi level in *Pnma* are of character similar to those in *I*4/*mmm* (see the SI); i.e., the metallic character of *Pnma* is due to the π^*/σ^* overlap. We note that metallization of ionic compounds by band overlap at pressure has already been observed (e.g., in CsI[32] and BaTe[33]), although one has to remember that "ionic" $[XeF]^+F^-$ is also quite covalent as far as one looks at Xe−F bonding within the $[XeF]^+$ cation.

CONCLUSIONS

In this work, we examined theoretically the evolution of XeF_2 structures under pressure. We find that the ambient-pressure structure of xenon difluoride (*I*4/*mmm*) persists as the most stable form up to 105 GPa and that at this pressure it still can be described as a molecular crystal. Our results thus disagree with previous experimental findings,[10] which indicate that XeF_2 should exhibit four phase transitions up to 100 GPa. The structures derived from experimental studies turn out to be thermodynamically unfavorable and dynamically unstable in calculations. The discrepancies between theory and experiment, together with possible difficulties that may be encountered during the interpretation of PXRD patterns for Xe compounds, call for more accurate high-pressure structural investigations on xenon difluoride.

We find that above 105 GPa a *Pnma* structure (evolving to a higher symmetry *Cmcm*) becomes thermodynamically favored. This polymorph can be derived from *I*4/*mmm* by movement of half of the F atoms present in the unit cell, a displacement that results (in the regime of 105−150 GPa) in Xe−F bond asymmetry and bending of the XeF_2 unit and signal XeF_2 self-dissociation. Indeed, analysis of the ELF and electronic structure of *Pnma* (*Cmcm*) at 200 GPa indicates that this polymorph is best described as an ionic solid (i.e., $[XeF]^+F^-$), exhibiting a distorted anti-NiAs structure type. The high-pressure self-dissociation of XeF_2 is thus similar to that observed for compressed N_2O.

COMPUTATIONAL DETAILS

Our approach is based on the plane-wave-basis DFT, a current method of choice for calculation of the structures and properties of periodic crystals. Calculations utilized the Perdew−Burke−Ernzerhof exchange-correlation functional,[34] which has been successfully applied in the study of compressed CO_2.[35] The projector-augmented-wave method[36] was used, as implemented in the VASP 4.6 code.[37] The cutoff energy of the plane waves was set to 800 eV with a self-consistent-field convergence criterion of 1×10^{-7} eV. Valence electrons (F, 2s and 2p; Xe, 5s and 5p) have been treated explicitly, while standard VASP pseudopotentials (accounting for scalar relativistic effects) were used for the description of core electrons. The *k*-point mesh was generated for every structure in such a way that the spacing between the *k* points was approximately 0.14 $Å^{-1}$. Structures have been optimized using a conjugate-gradient algorithm with a convergence criterion of 1×10^{-6} eV. This ensured that in the optimized structures forces acting on the ions were smaller than 2 meV/Å. We have checked the validity of our calculations by comparing them with ambient-pressure structure data of XeF_2 and F_2 (see the SI). The enthalpy derived from our calculations does not contain the zero-point-energy (ZPE) correction. We found that the difference in the ZPE between *I*4/*mmm* and *Pnma* does not exceed 10 meV per XeF_2 unit in the whole pressure range studied.

The direct method, as implemented in *PHONON*,[38] was used for calculation of the phonon dispersion curves and phonon DOSs. The units cells of *I*4/*mmm*, *Pnma*/*Cmc*2_1, *Fmmm*, and *Pnnm*-2 were expanded into supercells with vector lengths of around 10 Å. Energy calculations for the supercells generated by *PHONON* were done using VASP. Because of the large number of atoms in the supercells (up to 144 for *Pnma*/*Cmc*2_1), we were forced to loosen the calculation parameters by choosing a cutoff energy of 600 eV, a *k*-point spacing of 0.2 $Å^{-1}$, and a convergence criterion for forces of 1 meV/Å.

The *I*4/*mmm* polymorph exhibits no imaginary modes from 0 to 200 GPa; *Pnma* is dynamically stable from 105 to 200 GPa. Calculation of the phonon dispersion curve for *Cmc*2_1 at 150 and 175 GPa indicates that this polymorph exhibits an imaginary mode, which transforms it into *Pnma*. The *Fmmm* structure is dynamically unstable at 80 and 150 GPa;

dx.doi.org/10.1021/ic200371a |*Inorg. Chem.* 2011, 50, 3832–3840

it collapses to the *I*4/*mmm* polymorph as soon as the symmetry constraint is waived. *Pnnm*-2 exhibits imaginary modes at 10 GPa. When optimized at pressures higher than 15 GPa, it collapses to *I*4/*mmm* even without lifting the symmetry constraints of the *Pnnm* space group.

The structural drawings presented in this work have been made with the use of the *VESTA* program.[39]

■ ASSOCIATED CONTENT

Supporting Information. Summary of XeF_2 polymorphs studied, evolution of Xe···F and F···F contacts with pressure, structure parameters and enthalpy of selected polymorphs, electronic band structure and density of states, and test calculations. This material is available free of charge via the Internet at http://pubs.acs.org.

■ AUTHOR INFORMATION

Corresponding Author

*E-mail: dkurzydlowski@chem.uw.edu.pl. Fax: +48-22-5540800.

■ ACKNOWLEDGMENT

D.K.'s stay at Cornell University was supported by the National Science Foundation within Contract CHE-0910623. W.G. and D.K. acknowledge support for this research from the Foundation for Polish Science "TEAM" Programme cofinanced by the EU European Regional Development Fund.

■ DEDICATION

This work celebrates the 400th anniversary of the birth of Johannes Hevelius, eminent Polish astronomer.

■ REFERENCES

(1) Bartlett, N. *Proc. Chem. Soc., London* **1962**, 218.

(2) Lehmann, J. F.; Mercier, H. P. A.; Schrobilgen, G. J. *Coord. Chem. Rev.* **2002**, *233*, 1–39. Holloway, J. H.; Hope, E. G. *Adv. Inorg. Chem.* **1999**, *46*, 51–100. Grochala, W. *Chem. Soc. Rev.* **2007**, *36*, 1533–1696.

(3) Tramšek, M.; Žemva, B. *Acta Chim. Slov.* **2006**, *53*, 105–116.

(4) (a) Levy, H. A.; Agron, P. A. *J. Am. Chem. Soc.* **1963**, *85*, 241–242. (b) Agron, P. A.; Begun, G. M.; Levy, H. A.; Mason, A. A.; Jones, C. G.; Smith, D. F. *Science* **1963**, *139*, 842–844. (c) Siegel, S.; Gebert, E. *Chem. Commun.* **1963**, *85*, 240. (d) Elliot, H. S. A.; Lehmann, J. F.; Mercier, H. P. A.; Jenkins, H. D. B.; Schobilgen, G. J. *Inorg. Chem.* **2010**, *49*, 8504–8523.

(5) Gillespie, R. J.; Robinson, R. J. *Angew. Chem., Int. Ed. Engl.* **1996**, *35*, 495–514.

(6) Pimentel, G. C. *J. Chem. Phys.* **1951**, *19*, 446–448. Hach, R. J.; Rundle, R. E. *J. Am. Chem. Soc.* **1951**, *73*, 4321–4324. Rundle, R. E. *J. Am. Chem. Soc.* **1963**, *85*, 112–113. Munzarová, M. L.; Hoffmann, R. *J. Am. Chem. Soc.* **2002**, *124*, 4787–4795.

(7) Bagus, P. S.; Liu, B.; Liskow, D. H.; Schaefer, H. F., III *J. Am. Chem. Soc.* **1975**, *97*, 7216–7219. For more recent calculations on XeF_2, see: Liao, M.-S.; Zhang, Q.-E. *J. Phys. Chem. A* **1998**, *102*, 10647–10654. Grant, D. J.; Wang, T.-H.; Dixon, D. A.; Christe, K. O. *Inorg. Chem.* **2010**, *49*, 261–270. Dixon, D. A.; de Jong, W. A.; Peterson, K. A.; Christe, K. O.; Schrobilgen, G. J. *J. Am. Chem. Soc.* **2005**, *127*, 8627.

(8) Coulson, C. A. *J. Chem. Phys.* **1966**, *44*, 468–469.

(9) (a) Sladky, F. O.; Bulliner, P. A.; Bartlett, N. *J. Chem. Soc. A* **1969**, 2179. (b) Bartlett, N.; Wechsberg, M.; Jones, G. R.; Burbank, R. D. *Inorg. Chem.* **1972**, *11*, 1124–1127. (c) Bartlett, N.; Gennis, M.; Gibler, D. D.; Morell, B. K.; Zalkin, A. *Inorg. Chem.* **1973**, *12*, 1717–1721. (d) Zalkin, A.; Ward, D. L.; Biagoni, R. N.; Tempelton, D. H.; Bartlett, N. *Inorg. Chem.* **1978**, *17*, 1318–1322.

(10) Kim, M.; Debessai, M.; Yoo, C.-S. *Nat. Chem.* **2010**, *2*, 784–788.

(11) The authors report that phase III has the same symmetry as phase IV with different ordering of the atoms. Therefore, in order to distinguish them, they mark the former as *Pnnm*-1 and the latter as *Pnnm*-2.

(12) Burbank, R. D.; Falconer, W. E.; Sunder, W. A. *Science* **1972**, *178*, 1285–1286.

(13) For a list of all structures studied, see the SI.

(14) Santoro, M.; Gorelli, F. A. *Chem. Soc. Rev.* **2006**, *35*, 918–931 and references cited therein.

(15) (a) Somayazulu, M.; Madduri, A.; Goncharov, A. F.; Tschauner, O.; McMillan, P. F.; Mao, H.-k.; Hemley, R. J. *Phys. Rev. Lett.* **2001**, *87*, 135504-1–135504-1. (b) Yoo, C. S.; Iota, V.; Cynn, H.; Nicol, M.; Park, J.-H.; Le Bihan, T.; Mezouar, M. *J. Phys. Chem. B* **2003**, *107*, 5922–5925. (c) Song, Y.; Somayazulu, M.; Mao, H.-k.; Hemley, R. J.; Herschbach, D. R. *J. Chem. Phys.* **2003**, *118*, 8350–8356. (d) Iota, V.; Park, J.-H.; Yoo, C. S. *Phys. Rev. B* 2004, *69*, 064106-1–064106-6.

(16) Oganov, A. R.; Glass, C. W. *J. Chem. Phys.* **2006**, *124*, 244704-1–244704-15. Oganov, A. R.; Glass, C. W.; Ono, S. *Earth Planet. Sci. Lett.* **2006**, *241*, 95–103. Glass, C. W.; Oganov, A. R.; Hansen, N. *Comput. Phys. Commun.* **2006**, *175*, 713–720.In our calculations, we used up to four XeF_2 molecules per unit cell.

(17) Volume per XeF_2 molecule at 50 GPa: 38.6 Å^3 (*I*4/*mmm*), 38.7 Å^3 (*Cmca*), and 44.5 Å^3 ($Pa\bar{3}$).

(18) The transformation between the face centered cell of *I*4/*mmm* and *Pnnm*-2 ($Z = 4$) and the standard cell ($Z = 2$) is simple with the cell vectors **a**, **b**, and **c** of the face centered cell equal respectively to $\mathbf{a}' + \mathbf{b}'$, $\mathbf{a}' - \mathbf{b}'$, and $\mathbf{c}'$, where $\mathbf{a}'$, $\mathbf{b}'$, and $\mathbf{c}'$ are the original vectors of the standard cell.

(19) An important experimental issue when dealing with XeF_2 is its stability with respect to decomposition into Xe and F_2. Kim et al. did not find signs of such a reaction taking places at high pressure.[10] Indeed, our calculations indicate that the enthalpy of decomposition of solid XeF_2 to solid Xe and F_2 is positive and equal to 144 kJ/mol at 0 GPa (compared to 151 kJ/mol found experimentally): Johnson, G. K.; Malm, J. G.; Hubbard, W. N. *J. Chem. Thermodyn.* **1972**, *4*, 879–891. It increases to 358 kJ/mol at 100 GPa because of the positive sign of the $p\Delta V$ term (for details, see the SI).

(20) Additionally, the Xe layers (expanding in the **a**−**b** plane) become slightly puckered, and the **a** and **b** cell vectors are differentiated (**a** lengthens and **b** becomes smaller), while **c** expands (see the SI).

(21) Bürger, H.; Kuna, R.; Ma, S.; Breidung, J.; Thiel, W. *J. Chem. Phys.* **1994**, *101*, 1–14. We note that the low frequencies of those vibrations result partly in the large reduced mass of the XeF_2 oscillator.

(22) For pressure evolution of the Xe···F and F···F contacts in the *I*4/*mmm* and *Pnma* structures, see the SI.

(23) Häussermann, U.; Berastegui, P.; Carlson, S.; Haines, J.; Léger, J.-M. *Angew. Chem.* **2001**, *113*, 4760–4765.

(24) The anti-NiAs structure type has been observed as one of the high-pressure phases of AgF: Hull, S.; Berastegui, P. *J. Phys.: Condens. Matter* **1998**, *10*, 7945–7955.

(25) Oganov, A. R.; Chen, J.; Gatti, X.; Ma, Y.; Ma, Y.; Glass, C. W.; Liu, Z.; Yu, T.; Kurakevych, O. O.; Solozhenko, V. L. *Nature* **2009**, *457*, 863–868.

(26) Pickard, C. J.; Needs, R. J. *Nat. Mater.* **2008**, *7*, 775–779.

(27) Grochala, W.; Kriatchev, L.; Räsänen, M. . In *Physics & Chemistry at Low Temperatures*; Kriatchev, L., Ed.; Pan Stanford Publishing: Singapore, 2011; p 421.

(28) Bürgi, H. B.; Dunitz, J. D. *Acc. Chem. Res.* **1983**, *16*, 153–161.

(29) Jenkins, H. D. B.; Roobotoom, H. K.; Passmore, J. *Inorg. Chem.* **2003**, *42*, 2886–2893.

(30) Christe, K. O.; Dixon, D. A.; McLemore, D.; Wilson, W. W.; Sheehy, J. A.; Boatz, J. A. *J. Fluorine Chem.* **2000**, *101*, 151–153.

(31) Silvi, B.; Savin, A. *Nature* **1994**, *371*, 683–686. Savin, A.; Jepsen, A.; Flad, J.; Andersen, O. K.; Preuss, H.; von Schnering, H. G. *Angew. Chem., Int. Ed. Engl.* **1992**, *31*, 187–188.

(32) Eremets, M. I.; Shimizu, K.; Kobayashi, T. C.; Amaya, K. *Science* **1998**, *281*, 1333–1335.
(33) Grzybowski, T. A.; Ruoff, A. L. *Phys. Rev. Lett.* **1984**, *53*, 489–492.
(34) Perdew, J. P.; Burke, K.; Ernezrhof, M. *Phys. Rev. Lett.* **1997**, *77*, 3865–3868.
(35) Bonev, S. A.; Gygi, F.; Ogitsu, T.; Galli, G. *Phys. Rev. Lett.* **2003**, *91*, 065501-01–065501-04.
(36) Blöchl, P. E. *Phys. Rev. B* **1994**, *50*, 17953–17979.
(37) Kresse, G.; Futhmüller, J. *Phys. Rev. B* **1996**, *54*, 11169–11186. Kresse, G.; Futhmüller, J. *Comput. Mater. Sci.* **1996**, *6*, 15–50. Kresse, G.; Joubert, D. *Phys. Rev. B* **1999**, *59*, 1758–1775.
(38) Parliński, K.; Li, Z. Q.; Kawazoe, Y. *Phys. Rev. Lett.* **1997**, *78*, 4063–4066.
(39) Momma, K.; Izumi, F. *J. Appl. Crystallogr.* **2008**, *41*, 653–658.